High-Sensitivity Gas Sensor Based on Suspended Core Subwavelength Fiber

Luan Nannan Wang Ran Hao Congjing Yuan Cai Lu Ying Yao Jianquan

(*Key Laboratory of Opto-Electronics Information Technology, Ministry of Education, College of Precision Instrument and Opto-Electronics Engineering, Tianjin University, Tianjin*, 300072, *China*)

Abstract A suspended-core fiber (SCF) with subwavelength core diameter is numerically analyzed for gas sensing application. The dependence of the relative sensitivity, effective mode area, and confinement loss on the fiber parameters as well as the refractive index of fiber material is investigated with finite element method. The simulation results show that the relative sensitivity and confinement loss will increase with the decrease of the core diameter and the fiber refractive index. The effective mode area decreases at first, and then increases when the fiber core decreases to a certain value. The confinement loss decreases dramatically with the increase of the air hole diameter, while the relative sensitivity and effective mode area remain unchanged. These results prove that the proposed SCF with subwavelength core diameter is very promising for developing a high-sensitivity gas sensor with large effective mode area and low confinement loss.

Key words fiber optics; sensors; microstructured optical fiber; gas sensor; suspended core fiber; evanescent field

OCIS codes 060.4005; 060.2310; 060.2370; 280.4788

基于亚波长悬浮芯光纤的高灵敏度气体传感器

栾楠楠 王 然 郝丛静 袁 偲 陆 颖 姚建铨

(天津大学精密仪器与光电子工程学院光电子信息技术科学教育部重点实验室, 天津 300072)

摘要 数值分析了亚波长悬浮芯光纤在气体传感方面的应用。利用有限元法研究了相对灵敏度、有效模场面积、限制损耗与光纤参数包括纤芯直径和光纤材料折射率之间的关系。结果显示,相对灵敏度和限制损耗随着纤芯直径和光纤材料折射率的降低而增加。随着纤芯直径的减小,有效模场面积出现了先减小后增加的现象。增加包层孔直径能有效降低限制损耗,而相对灵敏度和有效模场面积保持不变。这些结果证明,亚波长悬浮芯光纤非常适合成为高灵敏度、大有效模场面积、低限制损耗的气体传感器。

关键词 光纤光学; 传感器; 微结构光纤; 气体传感器; 悬浮芯光纤; 倏逝场

中图分类号 O439 **文献标识码** A **doi**: 10.3788/CJL201441.0514001

1 Introduction

Microstructured optical fibers (MOFs) or photonic crystal fibers (PCFs) that incorporate air holes within their cross-section offer numerous new characteristics and opportunities for many sensing applications[1-4]. The holes within MOFs can be used to control the interactions between guided light and gas located within the holes while simultaneously acting as tiny sample chambers[1-2]. Two types of guidance are possible in these fibers: hollow core fibers guiding by photonic bandgap (photonic bandgap fibers (PBFs)) or solid core fibers guiding by total internal reflection (index-guiding MOFs).

In PBFs, the light is confined within the air core by a two-dimensional photonic bandgap formed by the periodic structure of the cladding allowing transmission over a limited wavelength range. It has been shown that in PBFs more than 98% of the guided mode field energy can propagate in the air regions of the fiber, which causes an increase in the interaction[5-7]. However, the PBFs have two main significant drawbacks, one of which is a limited spectral range, typically narrower

收稿日期: 2013-10-31; **收到修改稿日期**: 2013-11-25

基金项目: 国家 973 计划(2010CB327801)

作者简介: 栾楠楠(1985—),男,博士研究生,主要从事光子晶体光纤传感方面的研究。E-mail: lsouthwood@sina.com

导师简介: 姚建铨(1939—),男,教授,博士生导师,主要从事激光与非线性光学方面的研究。E-mail: jqyao@tju.edu.cn

than 100 nm for the bandgap effect. Thus, the PBFs are very well suited for a narrow-band chemical sensing. Another defect is that the periodic microstructure requires the precise and stringent control for the generated photonic bandgap. In order to avoid these limitations, some researchers used the evanescent field based on the index-guiding MOFs[8-10]. In these fibers, light penetrates holes as an evanescent field, hence only a small fraction of the total power (typically no more than 10%) is transmitted through the holes.

A particular example of the index-guiding MOFs is a suspended-core fiber (SCF)[11]. The fiber consists of a silica rod that has a diameter comparable with the light wavelength (about 1 μm) suspended with thin (on the order of a hundred nanometers) struts attached to a solid cladding of the fiber. Since the struts are much longer than the core diameter, the core is surrounded by large air-holes. Due to the large refractive index contrast between the solid core and the air-holes, light is confined in the core and typically a few percent of its total power penetrates the holes as an evanescent wave[12-13]. When the size of the core is smaller than the wavelength (typically less than 1 μm), towards the nanowire regime, the guided light is no longer predominantly confined to the core. The small core diameter that has been reported in the literature to date is several hundred nanometers[14-16], and light guided along such a nanowire leaves a large fraction of the guided field outside the wire as evanescent waves. Also, such a small core diameter offers a smaller mode area. It is well known that small mode area is a disadvantage for the coupling between light source and fiber. Moreover, moving to even-smaller core dimensions, given that the loss increases dramatically in this regime[15], limits the interaction length between light and gas via evanescent field effects.

For larger (larger than 2 μm) core SCFs, the fiber loss tends towards the material loss, indicating that fabrication, confinement and scattering losses are negligible[17]. In the small-core fiber regime under consideration here, the losses are significantly higher. There are two key reasons why loss increases as one scales down a fiber core. The first loss mechanism that can impacts small-core SCFs is confinement loss which is eliminated when the number of air-holes in cladding is infinite. Nevertheless, in the practical structure, the number of air-holes is finite. Thus confinement loss can be essentially eliminated via appropriate fiber design. The second loss mechanism that impacts small-core SCFs is scattering associated with surface roughness on the core interface[18]. Unlike confinement loss, there is no straightforward way of mitigating this loss mechanism, and thus it is thought to be the ultimate loss limitation of these small-core structures.

In this paper, we propose to use the SCF with subwavelength core diameter as single-mode waveguide in evanescent-wave-based optical gas sensor. The relationship between the gas sensing properties and the fiber parameters is discussed. We investigate the effects of changes in the diameter of the core, the size of cladding hole, and the refractive index of material on the relative sensitivity, effective mode area, and confinement loss.

2　Numerical simulation and analysis

Figure 1 shows the proposed SCF with the subwavelength core diameter, and the strut's thickness t_s is 200nm. The fiber is characterized by three important parameters: the core diameter d_c, the hole diameter d and the index of cladding material n.

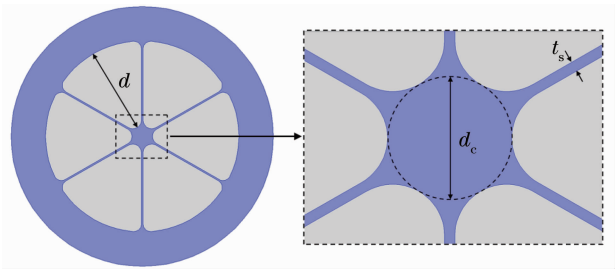

Fig. 1　Cross-section of the SCF

In our simulation study, we consider here the fundamental mode in the SCF. The guided light power is confined within the solid core region with a part (evanescent field) of power extended into the holey region. Relative sensitivity coefficient (r) at a particular wavelength is represented by[19]

$$r = (n_r/n_e)f, \tag{1}$$

where n_r is the index of the gas species and is approximately equal to 1, n_e is the effective index of the guided mode, f is the fraction of the total power located in the holes and can be calculated by integrating the optical power inside the air-holes and dividing it by the total power of the mode, and is expressed as[19]

$$f = \frac{\int_{\text{hole}} (E_x H_y - E_y H_x)\,\mathrm{d}x\mathrm{d}y}{\int_{\text{total}} (E_x H_y - E_y H_x)\,\mathrm{d}x\mathrm{d}y}, \tag{2}$$

where E_x, E_y and H_x, H_y are the transverse electric and magnetic fields of the mode. The effective index n_e and the mode field pattern (E_x, E_y and H_x, H_y) can be calculated by solving Maxwell's equations with finite element software (COMSOL Multiphysics).

The confinement loss L_c is proportional to the imaginary part of the effective index according to the relation[20]

$$L_c = 8.686 k_0 \,\mathrm{Im}[n_e], \tag{3}$$

where $k_0 = 2\pi/\lambda$ is the wavenumber with λ being the free-space wavelength.

The effective mode area A_{eff} is an important parameter in the context of source-to-fiber coupling and

could be calculated by using the following definition[21]:

$$A_{\mathrm{eff}} = \left(\int_S |E_t|^2 \mathrm{d}x\mathrm{d}y\right)^2 \Big/ \left(\int_S |E_t|^4 \mathrm{d}x\mathrm{d}y\right), \quad (4)$$

where E_t is the transverse electric field vector of the mode and S denotes the whole fiber cross section. The transverse electric field vector E_t is also calculated by solving Maxwell's equations with COMSOL Multiphysics software.

To date, the SCFs have been made from a range of glasses, including silica[22-23], lead silicate[15,24] and bismuth[25] glasses. In this work, the refractive index of materials (n) are considered to be equal to 1.45 (silica), 1.62 (F2 glass), 1.88 (SF57 glass) and 2.05 (bismuth glasses). The operating wavelength λ is taken as 1.65 μm, corresponding to an absorption line of methane gas[18].

3 Results

To investigate the dependence of the relative sensitivity, effective mode area, and confinement loss on the core diameter and refractive index of the SCF, we design a fiber with d = 3 μm. The relative sensitivity, effective mode and confinement loss as functions of the core diameter d_c for four different glasses at a wavelength of 1.65 μm are shown in Figs. 2 (a) ~ (c), respectively. The curves of relative sensitivity, effective mode area and confinement loss shift upward corresponding to a decrease in the refractive index of material. The relative sensitivity and confinement loss will increase as d_c and n decrease. As shown in Fig. 2(b), the effective mode area decreases at first, and then increases dramatically as d_c decreases to a certain value. From Fig. 2(c), it is seen that the confinement loss increases with the decrease of the core diameter, especially for the low refractive index. Note that as d_c decreases to a certain value, both L_c and A_{eff} increase sharply. This phenomenon is due to the fact that the fundamental mode is confined more weakly when the core decreases to the smaller diameter, which makes confinement loss and effective mode area increase dramatically. To understand it more clearly, the patterns of fundamental mode of the SCF with silica are shown in Fig. 3. As seen from the figure, fundamental mode distribution, corresponding to the effective mode area of the mode field, obviously increases with the decrease of core diameter at first (from 1.4 μm to 0.8 μm), and then increases when the core diameter decreases to a smaller value (from 0.8 μm to 0.4 μm). The penetration of the mode field into cladding, corresponding to the relative sensitivity, obviously increases with the decrease of core diameter, as shown in Fig. 3. The features may be exploited to enhance enormously the relative sensitivity and the effective mode area of the SCF.

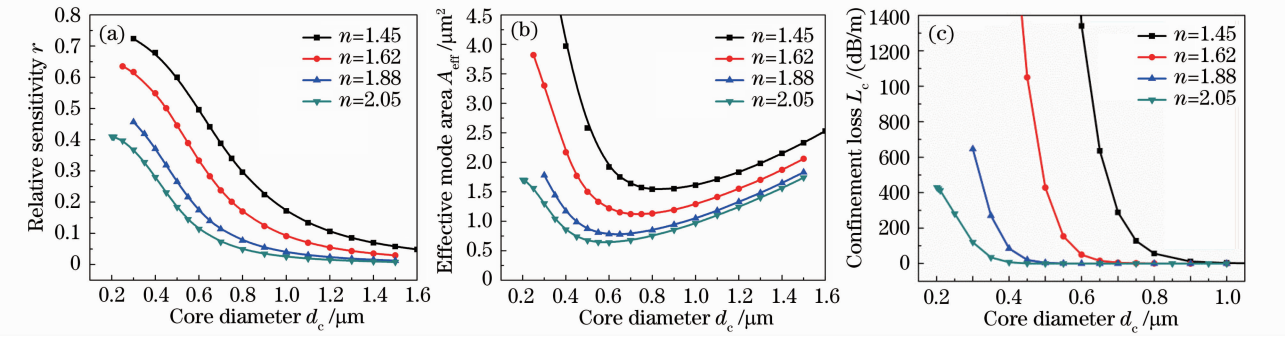

Fig. 2 (a) Relative sensitivity, (b) effective mode area and (c) confinement loss as functions of core diameter d_c for d = 3 μm with four different glasses at a wavelength of 1.65 μm

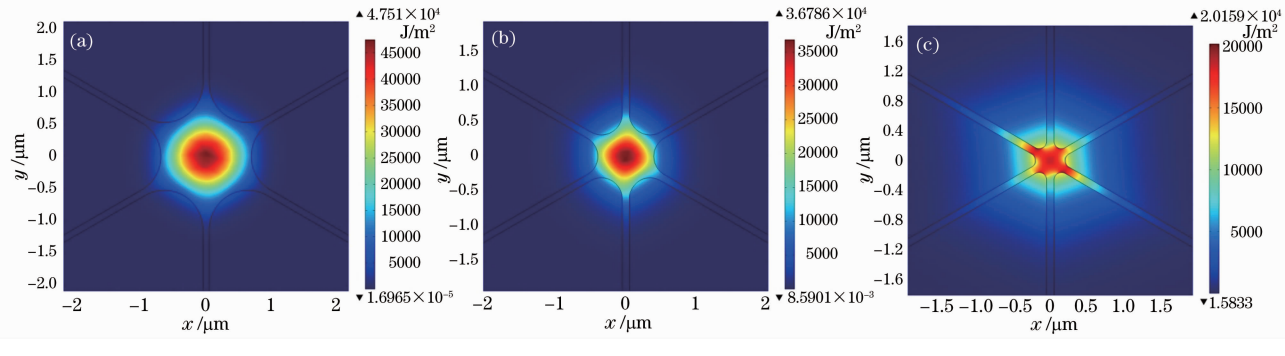

Fig. 3 Simulated distributions of the silica (n = 1.45) MOF fundamental modes with different diameter d_c of (a) 1.4 μm, (b) 0.8 μm, (c) 0.4 μm

In order to investigate the dependence of the relative sensitivity, effective mode area and confinement loss on the hole diameter and refractive index of the SCF, we examine a fiber with d_c = 0.3 μm which simultaneously

achieves more relative sensitivity and larger mode area. Figure 4 shows the relative sensitivity, effective mode area and confinement loss as functions of hole diameter d for $d_c = 0.3$ μm with four different glasses at a wavelength of 1.65 μm. It can be seen from Figs. 4(a) and (b) that, there is no obvious change in the relative sensitivity and effective mode area with the increase of d. But the confinement loss decreases dramatically for larger value of d, as shown in Fig. 4(c). With an increase of the air-hole diameter, the confinement loss will reduce because the effective cladding index declines with increasing hole diameter, which further increases the index contrast between core and cladding, so that the guided light can be confined in the core region, and the confinement loss decreases. Furthermore, the large air-holes also can be easily filled with gas. These results prove that the proposed SCF with small core and large air-holes is very promising for developing a gas sensor with high sensitivity, large effective mode area and low confinement loss.

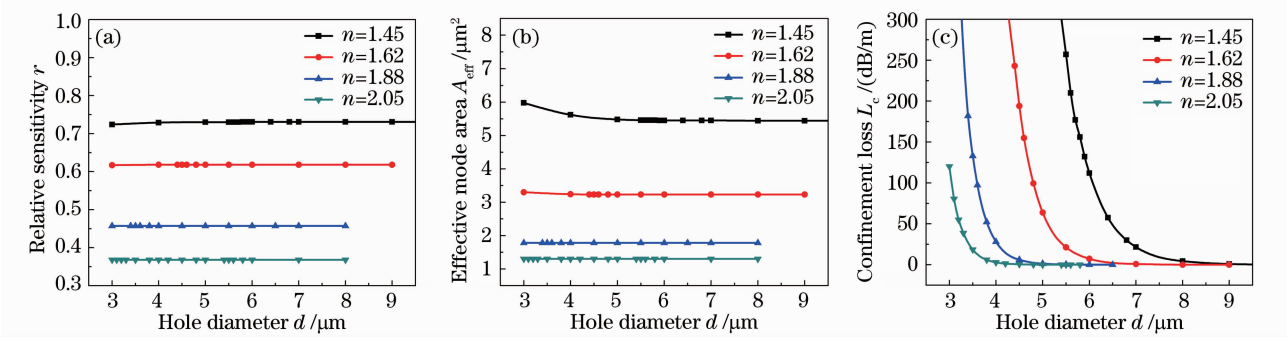

Fig. 4 (a) Relative sensitivity, (b) effective mode area and (c) confinement loss as functions of hole diameter d for $d_c = 0.3$ μm with four different glasses at a wavelength of 1.65 μm

4 Conclusion

We have demonstrated a gas sensor based on the SCF with subwavelength core diameter. The dependency of sensor properties such as the relative sensitivity, effective mode area and confinement loss on the fiber structural parameters and the refractive indices of fabrication material has been investigated. In the proposed fiber, the relative sensitivity and effective mode area have been improved by reducing diameter of the core and choosing low refractive index of material. Also, the confinement loss for our design has been decreased by increasing the air-hole size without reducing the relative sensitivity and effective mode area. Our numerical results indicate that, the proposed SCF with the subwavelength core diameter is very promising for developing a gas sensor with high sensitivity, large effective mode area and low confinement loss.

References

1 T M Monro, D J Richardson, P J Bennett. Developing holey fibers for evanescent field devices[J]. Electron Lett, 1999, 35(14): 1188 - 1189.

2 Y L Hoo, W Jin, H L Ho, *et al*.. Evanescent-wave gas sensing using microstructure fiber [J]. Opt Eng, 2002, 41(1): 8 - 9.

3 Yao Jianquan, Wang Ran, Miao Yinping, *et al*.. Novel photonic functional devices based on liquid-filling microstructured optical fibers[J]. Chinese J Lasers, 2013, 40(1): 0101002.
姚建铨，王　然，苗银萍，等. 基于液体填充微结构光纤的新型光子功能器件[J]. 中国激光，2013，40(1)：0101002.

4 Wu Tiesheng, Wang Li, Wang Zhe, *et al*.. A photonic crystal fiber temperature sensor based on Sagnac interferometer structure [J]. Chinese J Lasers, 2012, 39(11): 1114002.
伍铁生，王　丽，王　哲，等. 一种 Sagnac 干涉仪结构的光子晶体光纤温度传感器[J]. 中国激光，2012，39(11)：1114002.

5 S Smolka, M Barth, O Benson. Highly efficient fluorescence sensing with hollow core photonic crystal fibers[J]. Opt Express. 2007, 15(20): 12783 - 12791.

6 Y L Hoo, W Jin, J Ju, *et al*.. Numerical investigation of a depressed-index core photonic crystal fiber for gas sensing[J]. Sensor Actuat B-Chem, 2009, 139(2): 460 - 465.

7 Cheng Tonglei, Li Shuguang, Zhou Guiyao, *et al*.. Relation between power fraction in the core of hollow-core photonic crystal fibers and their bandgap property[J]. Chinese J Lasers, 2007, 34(2): 249 - 254.
程同蕾，李曙光，周桂耀，等. 空芯光子晶体光纤纤芯中的功率分数及其带隙特性[J]. 中国激光，2007，34(2)：249 - 254.

8 X Yu, Y C Kwok, N A Khairudin, *et al*.. Absorption detection of cobalt (Ⅱ) ions in an index-guiding microstructured optical fiber [J]. Sensor Actuat B-Chem, 2009, 137(2): 462 - 466.

9 C Martelli, J Canning, D Stocks, *et al*.. Water-soluble porphyrin detection in a pure-silica photonic crystal fiber[J]. Opt Lett, 2006, 31(14): 2100 - 2102.

10 J Park, S Lee, S Kim, *et al*.. Enhancement of chemical sensing capability in a photonic crystal fiber with a hollow high index ring defect at the center[J]. Opt Express, 2011, 19(3): 1921 - 1929.

11 A S Webb, F Poletti, D J Richardson, *et al*.. Suspended-core holey fiber for evanescent-field sensing [J]. Opt Eng, 2007, 46(1): 010503.

12 T Pustelny, M Grabka. Photonic-crystal fibres with suspended core: numerical analyses[J]. Acta Phys Pol A, 2008, 114(6-A): 115 - 120.

13 T Pustelny, M Grabka. Numerical investigation of the photonic-crystal fibres with suspended core[J]. Acta Phys Pol A, 2009, 116(3): 385 - 388.

14 W Q Zhang, V S Afshar, H Ebendorff-Heidepriem, *et al*.. Record nonlinearity in optical fibre[J]. Electron Lett, 2008, 44(25): 1453 - 1455.

15 H Ebendorff-Heidepriem, S C Warren-Smith, T M Monro. Suspended nanowires: fabrication, design and characterization of fibers with nanoscale cores [J]. Opt Express, 2009, 17(4): 2646 - 2657.

16 M Liao, C Chaudhari, X Yan, *et al*.. A suspended core nanofiber

with unprecedented large diameter ratio of holey region to core [J]. Opt Express, 2010, 18(9): 9088 - 9097.

17 H Ebendorff-Heidepriem, Y Li, T M Monro. Reduced loss in extruded soft glass microstructured fibre [J]. Electron Lett, 2007, 43(24): 1343 - 1345.

18 P J Roberts, F Couny, H Sabert, *et al*.. Loss in solid-core photonic crystal fibers due to interface roughness scattering[J]. Opt Express, 2005, 13(20): 7779 - 7793.

19 Y L Hoo, W Jin, C Shi, *et al*.. Design and modeling of a photonic crystal fiber gas sensor[J]. Appl Opt, 2003, 42(18): 3509 - 3515.

20 Y Lu, C Hao, B Wu, *et al*.. Surface plasmon resonance sensor based on polymer photonic crystal fibers with metal nanolayers [J]. Sensors, 2013, 13(1): 956 - 965.

21 M Koshiba, K Saitoh. Structural dependence of effective area and mode field diameter for holey fibers[J]. Opt Express, 2003, 11(15): 1746 - 1756.

22 Y K Lizé, E C Mägi, V G Ta′eed, *et al*.. Microstructured optical fiber photonic wires with subwavelength core diameter[J]. Opt Express, 2004, 12(14): 3209 - 3217.

23 L Dong, B K Thomas, L Fu. Highly nonlinear silica suspended core fibers[J]. Opt Express, 2008, 16(21): 16423 - 16430.

24 J Y Y Leong, P Petropoulos, J H V Price, *et al*.. High-nonlinearity dispersion-shifted lead-silicate holey fibers for efficient 1-μm pumped supercontinuum generation [J]. J Lightwave Technol, 2006, 24(1): 183 - 190.

25 H Ebendorff-Heidepriem, P Petropoulos, S Asimakis, *et al*.. Bismuth glass holey fibers with high nonlinearity [J]. Opt Express, 2004, 12(21): 5082 - 5087.

栏目编辑：殷建芳